Effect of Electrostatic Interactions and Dynamic Disorder on the Distance Dependence of Charge Transfer in Donor−Bridge−Acceptor Systems†

Ferdinand C. Grozema,‡ Yuri A. Berlin,§ Laurens D. A. Siebbeles,‡ and Mark A. Ratner*,§

Opto-electronic Materials Section, Department of Chemical Engineering, Delft University of Technology, Julianalaan 136, 2628 BL, Delft, The Netherlands, and Center for Nanofabrication and Molecular Self-Assembly, Department of Chemistry, Northwestern University, 2145 Sheridan Road, Evanston, Illinois 60208-3113

Received: March 15, 2010; Revised Manuscript Received: June 3, 2010

Using a tight-binding model of charge transport in systems with static and dynamic disorder, we present a theoretical study of the positive charge transfer in molecular assemblies that involve a hole donor and an acceptor connected by fluorene and phenyl bridges. Two parameters that determine the rate of charge transfer within the proposed model are the charge transfer integral between neighboring units and the site energies. Fluctuations in the values of the charge transfer integral and the energy landscape for hole transport were calculated by taking into account variations of the dihedral angle between neighboring units and electrostatic interaction of positive charge moving along the bridge and the negative charge that remains on the hole donor. Analysis of the dynamics of hole transfer and the distribution of the positive charge during this process allows the conclusion that the rapid fall of the hole transfer rate coefficient observed in experiments with short bridges (three and four structural units for systems with fluorene and phenyl bridges, respectively) can be attributed to the electrostatic interaction. This interaction is responsible for the formation of the effective barrier between donor and acceptor with the height that increases as the number of structural bridge units remains less than 3 (fluorene bridge) or 4 (phenyl bridge). For longer bridges, however, the effective barrier changes only weakly and now the charge transport is mostly dominated by the fluctuation-assisted incoherent hole migration along the bridge. The latter mechanism exhibits much weaker dependence of the rate coefficient on the bridge length in agreement with the available experimental results.

I. Introduction

There is currently an extensive interest in the study of mechanisms governing the process of photoinduced intramolecular charge transfer (CT) in molecular assemblies consisting of an electron (or hole) donor (D) and an acceptor (A) connected by a bridge (B). The number and variety of such donor−bridge−acceptor (D−B−A) systems have grown explosively in recent years. They can be divided roughly into those with π-bond conjugated bridges and those with σ-bonded bridges, although hybrid combinations are also known.[1] The increasing interest in various D−B−A molecules is much due to their potential use in molecular electronics,[2−5] solar cells,[6−10] and in artificial photosynthesis.[11−17] In addition, these molecules are widely used as convenient model systems for probing intramolecular charge transfer by different experimental techniques (for details, see refs 18−27).

Theoretical analysis of experiments on ET between donor and acceptor sites through bridges of different chemical structures reveals several basic mechanisms for the intramolecular nonresonant charge transfer process.[28] The existence of such mechanisms becomes most evident for bridges without static and/or dynamic disorder. In such simple D−B−A systems all the bridge sites are the same (that is, the site energies are all equal), and the electronic coupling between nearest neighbors is a single time-independent value, V. If the energy splitting of bridge states due to their electronic coupling does not reduce the energy gap $\Delta\varepsilon$ between the donor and the bridge states significantly, so that the inequality $\Delta\varepsilon/V \gg 1$ holds, a charge can be transferred from D to A via the single-step coherent tunneling without physical occupation of the bridge.[29] For this superexchange mechanism of coherent tunneling, one generally expects that the probability of transferring an electron/hole from D to A decreases exponentially with the length of the bridge R_{DA}, giving rise to an exponential distance dependence of the charge transfer rate coefficient k_{CT} (see, e.g., refs 29a−c and 29f)

$$k_{CT} = k_0 e^{-\beta R_{DA}} \tag{1}$$

where k_0 and β are the scaling factor and the falloff parameter, respectively.

However, if $\Delta\varepsilon/V \ll 1$, other regimes of CT are feasible. Since now the gap $\Delta\varepsilon$ effectively vanishes, electrons or holes can be transferred from D to A through long bridges undergoing the motion in a tight-binding band.[30] According to the Ioffe−Frohlich−Sewell criterion,[31] this mechanism of CT dominates if a particle with charge e and mass m has the intramolecular drift mobility $\mu_{im} > \mu^* = e\hbar/(4mV)$. In the opposite situation of slow mobility ($\mu_{im} \leq \mu^*$) the effects of polaronic on-site coupling become so significant that a charge will be temporarily localized on a bridge subunit and will move toward the acceptor in the incoherent regime of sequential hopping. Based on theoretical results[32] obtained for bridges with

† Part of the "Michael R. Wasielewski Festschrift".

* Address correspondence to any author. E-mail: F.C.G., F.C.Grozema@tudelft.nl; Y.A.B., berlin@chem.northwestern.edu; L.D.A., L.D.A.Siebbeles@tudelft.nl; M.A.R., ratner@chem.northwestern.edu.

‡ Delft University of Technology.

§ Northwestern University.

10.1021/jp1023422
Published on Web 06/24/2010

identical equienergetic hopping sites, the dependence k_{CT} vs R_{DA} in the hopping regime is usually approximated by the algebraic function, while the band-like charge transport in the weak scattering limit suggests that

$$k_{CT} \sim 1/R_{DA} \tag{2}$$

There is no dichotomy between coherent and incoherent mechanisms of charge transport. On the contrary, theoretical treatments have shown that each can contribute to the mechanism of the process. In the absence of disorder this leads to a characteristic form of the calculated dependence k_{CT} vs R_{DA} for hole transport; the rate coefficient of hole transfer rapidly falls as the number of bridge sites n is less than or equal to 3 and then decreases much slower for further elongation of the bridge.[33] This form of the distance dependence was indeed observed experimentally for a number of D−B−A molecular assemblies (see, e.g., refs 34−37). Furthermore, it has been found that the described behavior of k_{CT} as a function of R_{DA} is not restricted to the special case of bridges with equienergetic bridge sites.

To elucidate the main physical factors responsible for changes of k_{CT} with the bridge length in the more general case of D−B−A systems with static and dynamic disorder, we have theoretically studied hole migration in the molecular assemblies containing fluorene and phenyl bridges with the special emphasize on the effects of the electrostatic interaction and dynamic fluctuations on the rate of the hole transfer process. The analysis of computational results obtained shows that the rapid fall of the hole transfer rate coefficient for relatively short bridges (3 and 4 structural units for systems with fluorene and phenyl bridges, respectively) can be attributed to the electrostatic interaction between positive charge injected in the bridge and the negative charge that stays behind on the hole donor. As follows from the simulation data, this interaction leads to the formation an effective barrier between D and A with a height that increases as the number of structural bridge units in the system remains less than 3 (fluorene bridge) or 4 (phenyl bridge). For longer bridges, however, this effective barrier height changes only weakly and charge transport is mostly dominated by the fluctuation-assisted incoherent charge migration along the bridge. The latter mechanism of hole transfer exhibits much weaker dependence k_{CT} vs R_{DA} in agreement with experimental observations.

II. Computational Methods

We have studied charge transport in D−B−A systems theoretically by representing the molecules as a one-dimensional chain of planar conjugated units. Usually charge transfer in such systems is discussed in terms of a single step process through an intervening bridge. In this work we explicitly consider the energetic structure and disorder in the bridge during charge transfer. To do this, a whole sequence of charge transfer reactions along several bridge units has to be considered. The rate of each of these charge transfer reactions is characterized by a specific charge transfer integral and energy difference between the energies of the sites involved. To study the transfer of charges in a D−B−A system, we use a tight-binding model, which can take the variations in the energy difference and charge transfer integral along the sequence of bridge sites into account.[28,38,39] The wave function of the charge, $\Psi(t)$, at time t is taken to be a linear combination of basis functions, φ_n, that are localized on each subunit

$$\Psi(t) = \sum_{n=1}^{N} c_n(t)|\varphi_n\rangle \tag{3}$$

where $c_n(t)$ are expansion coefficients. In the case of hole migration through the D−B−A system the wave function of the positive charge can, to a good approximation, be expressed as a linear combination of the highest occupied molecular orbitals (HOMO) of the individual units. In typical experiments on D−B−A systems, a hole is usually created on the hole donor, e.g., by photoexcitation, and can be considered localized initially. This initial condition is satisfied in our simulations by setting the expansion coefficient on the donor site (c_1) equal to one at $t = 0$, while all others are taken to be zero. The motion of the charge carriers along the conjugated bridge, toward the acceptor, is simulated by propagating the wave function in time according to the time-dependent Schrödinger equation.

$$i\hbar\frac{\partial\Psi(t)}{\partial t} = \hat{H}\Psi(t) \tag{4}$$

The exact way in which the wave function evolves with time is determined by the Hamiltonian matrix (eq 5). The diagonal matrix elements of this matrix correspond to the site energies, $\varepsilon_{ii} = \langle\varphi_i|\hat{H}|\varphi_i\rangle$, that is, the energy of a charge carrier when it is localized on a single nucleobase (or the donor and acceptor). In the simplest approximation the site energies correspond to the ionization potential of a single isolated bridge unit (as well as the donor and the acceptor) if the transfer of positive charges is considered. In reality, this site energy will also depend for instance on the surrounding solvent.

When only nearest neighbor interactions are taken into account, the off-diagonal matrix elements of the Hamiltonian are equal to the charge transfer integral, $V_{ij} = \langle\varphi_i|\hat{H}|\varphi_j\rangle$, characterizing the electronic coupling between the HOMO orbitals on adjacent units, while all other off-diagonal matrix elements are zero. The Hamiltonian matrix is then given by

$$H = \begin{pmatrix} \varepsilon_{11} & V_{12} & 0 & \dots & 0 \\ V_{21} & \varepsilon_{22} & & & \\ 0 & & \ddots & & \\ \vdots & & & \ddots & \\ 0 & & & & \varepsilon_{NN} - \dfrac{i\hbar}{\tau} \end{pmatrix} \tag{5}$$

To ensure that the charge is irreversibly trapped when it arrives on the acceptor, a complex part is added to the diagonal matrix element of the acceptor site (N), $H_{NN} = \varepsilon_{NN} - i\hbar/\tau$. A decay time τ of 1 fs was used in the simulations described here. The value of τ was chosen small enough that the charge disappears from the last site instantaneously but not so small to cause reflections of the wave function on the last site. This ensures that the charge transfer rate that is obtained from the simulations is only determined by the propagation through the bridge and not by the value of τ. Variation of τ by a factor of 2 was not found to influence the results. The irreversible decay of the hole at the acceptor site leads to a decay of the total charge density on the D−B−A system.

The decay of the charge on the acceptor site leads to an overall decay of the amount of charge present, the so-called survival probability, $P(t)$. Experimentally, the rate of charge arrival at the acceptor defines the charge transfer rate, and

therefore, the decay of $P(t)$ corresponds to the formation of the charge-separated state. In the framework of the tight-binding description, the survival probability is defined as

$$P(t) = \sum_{n}^{N} |c_n(t)|^2 \tag{6}$$

The rate of arrival of the charge at the acceptor site, k_a, can be obtained from the decay of the survival probability in time since the charge decays very rapidly at the last site. This arrival rate is equivalent to the charge transfer rate, k_{CT}, defined in eqs 1 and 2. It should be noted that k_{CT} is sometimes used in experimental work to indicate the rate at which the hole leaves the hole donor, assuming single step charge transfer. Since the charge transfer does not necessarily occur in a single step, k_{CT} is not always the same as the rate at which the charge leaves the donor.[37]

The charge transfer integrals in eq 5 are very sensitive to the geometry of the D−B−A system. In the systems considered in this work the values of V strongly depend on the dihedral angle between neighboring units. In the work discussed here we initially sample these dihedral angles θ_i from a Boltzmann distribution based on the potential energy (U_{tor}) for rotation around θ,

$$P(\theta) = \frac{\exp\left(-\frac{U_{tor}(\theta)}{k_B T}\right)}{\int_0^{2\pi} \exp\left(-\frac{U_{tor}(\theta)}{k_B T}\right) d\theta} \tag{7}$$

where T is the temperature and k_B is Boltzmann's constant. The dihedral angles are generally not static during charge transfer, and therefore, the values of the torsion angles were propagated in time by assuming that the subunits in the bridge undergo rotational diffusion on the rotational potential energy profile discussed above. During a small time step, Δt, the change in the angles is given by[40]

$$\Delta\theta_i = -\frac{D_{rot}}{k_B T}\frac{\partial U_{tor}(\theta_i)}{\partial \theta_i}\Delta t + \Delta\theta_{dif} \tag{8}$$

The first term in eq 8 describes the rotational drift due to the torsion potential resulting from interaction of a given subunit with right and left neighbors, while the second term accounts for the random diffusive rotation. The value of the latter term is calculated according the relation $\Delta\theta_{diff} = (24 D_{rot}\Delta t)^{1/2}\chi$, with χ being a uniformly distributed random number in the interval, $[-1/2, 1/2)$ so that the mean squared value of $\Delta\theta_{diff}$ is given by

$$\langle \Delta\theta_{diff}^2 \rangle = 2 D_{rot}\Delta t \tag{9}$$

with $D_{rot} = 1/(2\tau_{rot})$ and τ_{rot} being the diffusional rotation time of the molecular subunits. The values of τ_{rot} for different molecules can be obtained from results of molecular simulations or can be measured by variety of techniques. Apart from the rotational degrees of freedom, there are many more internal degrees of freedom in the D−B−A systems considered. To achieve a perfect quantitative agreement with experimental data, these should be accounted for. However, as will be shown below, with the description of the rotations, the qualitative trends in the experimental data can be accounted for.

Different geometrical conformations will naturally also have their effect on the value of the site energies and introduce some disorder here too. In the cases considered here, the intramolecular charge transfer integrals are of the same order of magnitude or larger than the expected disorder in the site energies (<0.2 eV). Therefore, the effect of adding additional disorder is limited.

The combination of a quantum mechanical description of the charge with a classical propagation is in principle not in agreement with the detailed balance principle, especially when longer time scales are considered. In the systems treated in this work, the time scales are sufficiently short that this should not cause problems.

The charge transfer integrals were computed for different angles between two subunits using DFT with the fragment orbital approach as implemented in ADF. In this approach the orbitals of the $\pi-\pi$ stacked dimer are expressed as a linear combination of the molecular orbitals of the individual X-mer molecules. This procedure provides a direct and exact calculation of the charge transfer integrals and site energies.

III. Results and Discussion

As discussed in the preceding section, the main parameters that determine the rate of charge transfer in donor−bridge−acceptor systems are the charge transfer integrals and the site energies along the D−B−A system. We have studied the charge transfer in the two D−B−A systems shown in Figure 1. For these systems, experimental data from Wasielewski and coworkers are available.[34,35]

III.1. Torsion Potentials. To describe the disorder in the dihedral angles in the systems accurately, the dihedral potential, U_{tor}, has to be known. We have calculated the torsion potentials for the three angles in the D−B−A by ab initio calculations using Møller−Plesset perturbation theory and a cc-pVDZ basis set. The full geometry of a dimer consisting of the two subunits of interest was optimized while keeping only the dihedral angle fixed. The dihedral potentials obtained in this way are shown in Figure 2. In this figure only the data for D−B−A system A (fluorene) in Figure 1 are considered; however, the results for system B were found to be nearly identical. This can be understood since the local environments around the bond for which the dihedral potential is calculated are identical for the fluorene and phenyl units.

For the torsion potential of two fluorenes (see Figure 2a), the most stable configuration occurs at a dihedral angle close to 40°. At an angle of 0° a maximum is encountered with an energy that is 0.14 eV higher than the lowest energy conformation at a dihedral angle of about 45° where the potential energy is −0.14 eV relative to the potential energy for the planar dimer. For the torsion potential between a fluorene and the hole donor PDI shown in Figure 2b, a broad minimum is found around a dihedral angle of 90°. This suggests that angles between 60° and 120° are most likely. A similar picture is obtained for the torsion potential between a fluorene and the hole acceptor PTZ, as shown in Figure 2c. In this case the potential energy curve is rather shallow around 90°. Therefore, even though the equilibrium angle between the fluorene and the donor and acceptor are close to perpendicular, a range of dihedral angles will occur.

III.2. Charge Transfer Integrals. The charge transfer integrals in fluorene and phenyl dimers calculated as a function

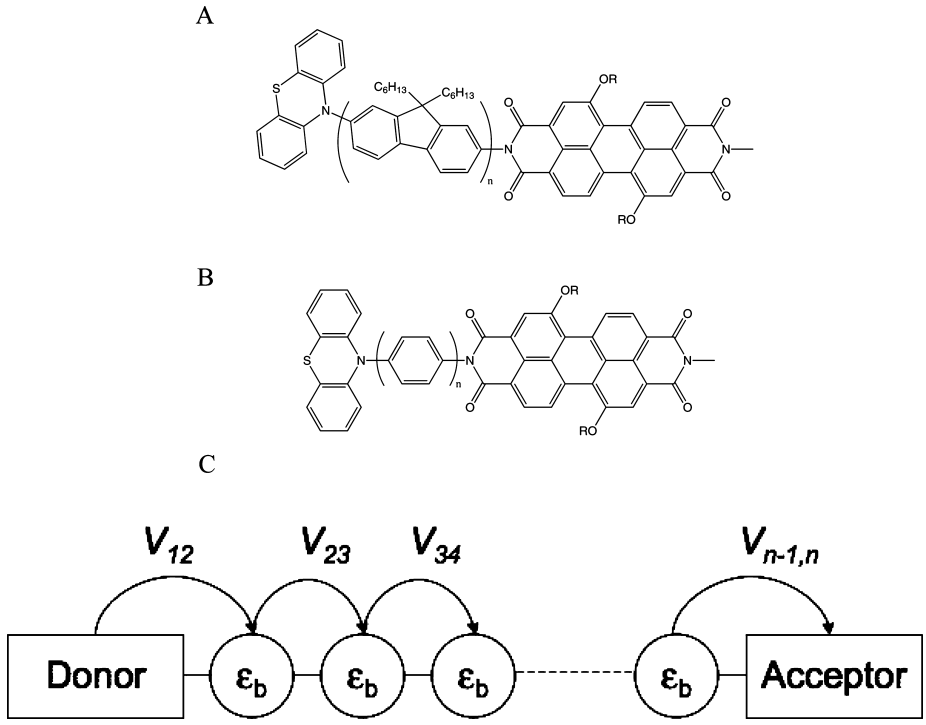

Figure 1. Molecular structure for D−B−A systems containing a fluorene (A) and a phenyl (B) bridge. In (C) the parameters for charge transfer are schematically indicated.

of the dihedral angle are shown in Figure 3. In both cases the charge transfer integral closely follows a cosine dependence, $V_{ij} = A\cos(\phi)$, with an amplitude A defining the maximum value of V. For biphenyl, the amplitude (0.75 eV) is considerably larger than for bifluorene (0.42 eV). This is due to the more delocalized nature of the HOMO orbital in fluorene. In a simple two-state model the orbitals on fluorene, which consists of two phenyl rings, would be bonding and antibonding combinations of the HOMO orbitals on both phenyls with a normalization constant of $1/\sqrt{2}$. This means that the charge transfer integral between two fluorenes would be lower than the charge transfer integral between two phenyls by a factor of 2 $(1/\sqrt{2})^2$. For the charge transfer integral between the donor and the bridge sites and between the bridge sites and the acceptor the charge transfer integral was also found to follow the cosine dependence. According to our calculations, the amplitude of this dependence is 0.34 and 0.45 eV for the charge transfer integral between fluorene and the hole donor and fluorene and acceptor, respectively. Both the coupling between the donor and phenyl and the coupling between the phenyl and acceptor were found to be roughly a factor $\sqrt{2}$ larger than for the coupling of the donor and acceptor to fluorene.

III.3. Site Energies. In most discussions of charge transfer in D−B−A systems the bridge is considered to be a rectangular barrier without any energetic structure (that is, all site energies are the same), or the bridge is described as a single unit.[35] In reality, both these approaches are not very accurate. An important problem lies in the fact that in many experiments, including the ones considered here, the injection of a positive charge in the bridge is accompanied by the formation of a negatively charge hole donor (in this case PDI^-). Therefore, the electrostatic interaction between the positive charge moving on, or tunneling through, the bridge and the negative charge that remains on PDI has to be taken into account. The value of ε_{ii} for a particular bridge site relative to the energy of the donor (ε_{11}) can be estimated using the following equation that is analogous to the Weller relation:[41,42]

$$\varepsilon_{ii} = E_{\text{ion}}(\text{B}) - E_{\text{el aff}}(\text{PDI}) - E_{\text{exc}}(\text{PDI}) - E_{\text{elst}}(\text{B}^+\text{PDI}^-) - \Delta E_{\text{solv}} \quad (10)$$

In this equation $E_{\text{ion}}(\text{B})$ denotes the ionization potential of the individual bridge units, while $E_{\text{el aff}}(\text{PDI})$ and $E_{\text{exc}}(\text{PDI})$ are the electron affinity and excitation energy of the hole donor, respectively. E_{elst} denotes the electrostatic interaction between the positive and negative charge, and ΔE_{solv} is the change in solvation energy upon charge separation. The latter two terms are discussed in more detail below. The sum of electron affinity $E_{\text{el aff}}(\text{PDI})$ and excitation energy, $E_{\text{exc}}(\text{PDI})$, of the hole donor corresponds to the electron affinity of the excited state of PDI. The sum of the first three terms in eq 10 gives the energy needed to make a transition from the excited state of PDI to the pair of oppositely charged ions PDI^-B^+ at infinite separation in vacuum. In reality, these charges are not at infinite distance in the D−B−A systems. Therefore, the (attractive) electrostatic interaction $E_{\text{elst}}(B^+PDI^-)$ at their actual distance should be subtracted. Finally, the stabilization of a charge-separated pair by the solvent is likely to be more than for the neutral system, especially in a polar solvent. This difference in solvation energy, ΔE_{solv}, should therefore, in principle, be taken into account in the values of ε_{ii}. The values for the ionization potential of the bridge unit, fluorene (benzene), are experimentally known and equal to 7.91 eV (9.24 eV). The electron affinity of the PDI unit containing two alkoxy groups as indicated in Figure 1 was calculated by density functional theory calculations and found to be equal to 2.48 eV. The first absorption band of the PDI is experimentally found at ∼550 nm, which is equal to 2.25 eV. The electrostatic interaction between PDI^- and B^+ was obtained by calculating the electrostatic interaction between two distributions of point charges, one for the PDI^- and one for a fluorene

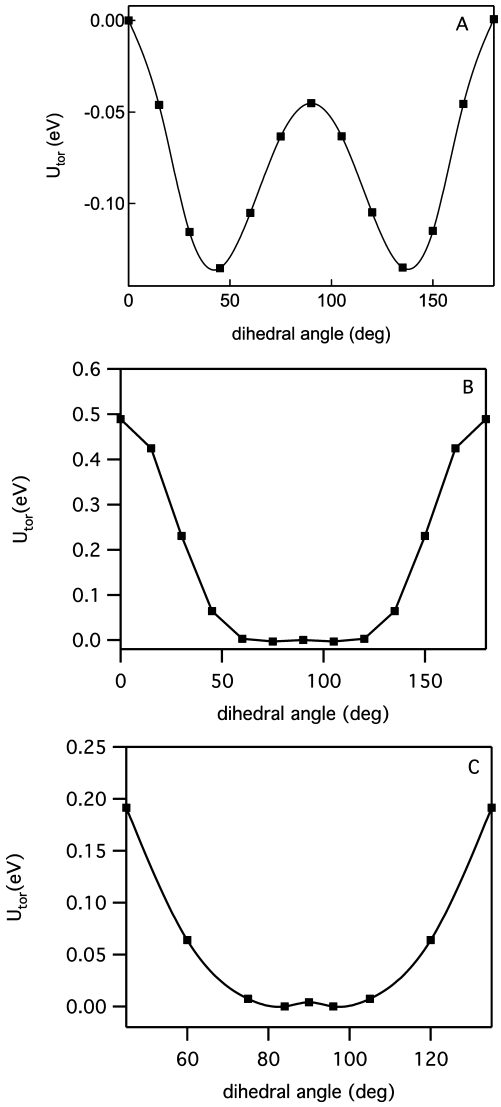

Figure 2. Torsion potential as a function of the dihedral angle for (A) two fluorenes, (B) a fluorene and the PDI hole-donor, and (C) a fluorene and the hole acceptor PTZ.

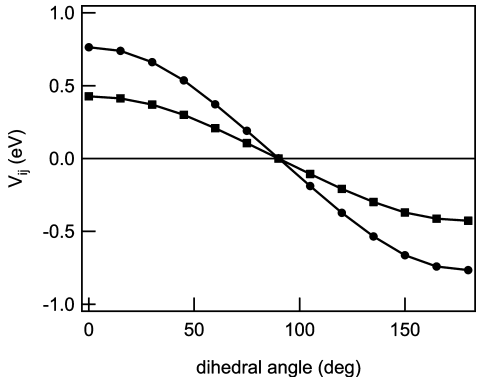

Figure 3. Charge transfer integral between two fluorene units (squares) and two phenyl units (circles) as a function of the dihedral angle.

(phenyl) at different positions along the D−B−A system. These point charges were obtained from a density functional theory calculation by fitting them to the electrostatic potential.[43] The solvent stabilization of the charge-separated pair was neglected in this case since the experiments on the D−B−A system considered were performed in apolar solvents. This is of course an approximation since even the surrounding polarizabilities due

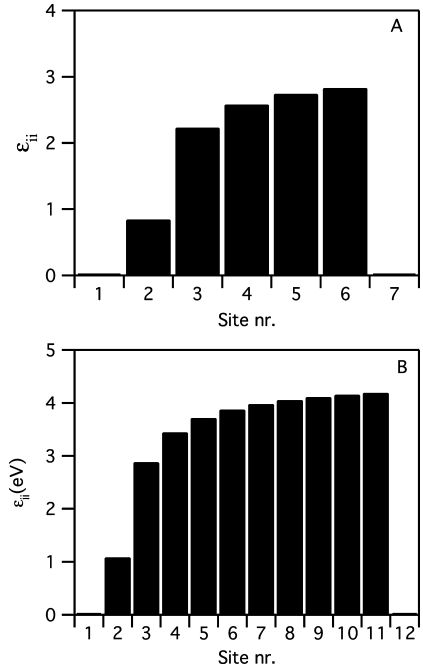

Figure 4. Site energy along the D−B−A system calculated using eq 10 for fluorene (A) and phenyl (B) bridges.

to the solvent molecules will screen the electrostatic interaction to some extent. The site energies that were obtained in this way are summarized in Figure 4 for the two D−B−A systems considered in this work. The site energies are shown for the longest systems considered, five fluorene units or 10 phenyl units. In the simulations, the site energy of the acceptor site was assumed to be the same as that of the hole. The site energies clearly reflect the electrostatic interaction between the positive charge on the bridge and the negative charge on the hole donor. The energy of the site next to the donor is in both cases considerably lower than the site energies further along the bridge since the electrostatic interaction is strongest here.

This way of assigning energies to individual bridge sites is rather different from the characterization of the entire bridge by a single energy value as sometimes assumed in theoretical analysis of the experimental results.[35] The bridge energies obtained in these two approaches differ significantly; the energy for a charge that is delocalized over the entire bridge is considerably lower than that for the individual bridge sites. It should be noted, however, that the actual energy of a delocalized charge on the bridge in the description with individual sites is much lower than that of the sites themselves because of the considerable charge transfer integral between the sites. Similarly, when the bridge is described as a single unit, the charge transfer integral between the donor and the bridge becomes smaller due to the more delocalized nature of the wave function of the charge on the bridge. This leads to a smaller amplitude of the wave function on the site next to the donor and hence a smaller charge transfer integral. Therefore, the higher site energies in the description with individual sites are compensated by the much larger charge transfer integrals. The advantage of a model with individual units is that it is possible to explicitly study systems in which not all site energies are the same. This can arise when there is disorder or when there is some systematic variation in the bridge energy due to different chemical structure of bridge units or, in this work, electrostatic interactions play a role.

III.4. Dynamics of Charge Transfer: Fluorene Bridge. The charge transfer between the donor and acceptor was simulated using the parameters discussed above. The rotation time for

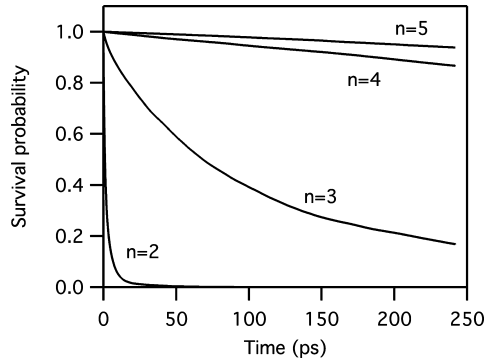

Figure 5. Survival probability as a function of time for D−B−A systems containing fluorene bridges of different lengths.

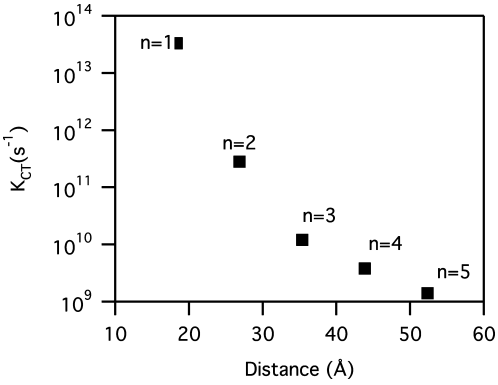

Figure 6. Charge transfer rate coefficient k_{CT} plotted against the distance between centers of donor and acceptor units in D−B−A systems with fluorene bridges.

rotational diffusion was taken to be 150 ps for all units in the D−B−A system. This is a typical value for molecules of similar sizes. Variation of this rotational diffusion time by a factor of 2 does not significantly influence the charge transfer rate obtained. Only when the rotation time is changed by an order of magnitude are differences observed. In this respect it is interesting to note that the time scale of the rotations is much longer than that of the charge transfer. Therefore, the bridge conformation is rather static during charge transfer and averaging of the charge transfer integrals over the angle is not a viable approach.[28] In Figure 5 the survival probability is shown for bridges consisting of 2−5 fluorenes. The decay curve for a bridge consisting of a single fluorene is not shown because it coincides with the vertical axis. It is clear from this figure that for the D−B−A systems consisting of 1−3 fluorene units the rate of charge transfer strongly decreases with increasing chain length. For the longer chains the dependence is much weaker. The rate of charge transfer was obtained from the curves in Figure 5 by fitting to an exponential. This resulted in reasonable fits for all chain lengths. The charge transfer rates are plotted against the chain length in Figure 6. As observed in the survival probability, the rate initially decreases rapidly with chain length, but for longer bridges levels off. For the bridges consisting of 3−5 fluorene units, the charge transfer rate decays exponentially with distance. The value for β derived from the exponential fit indicated in Figure 6 is 0.13 Å^{-1}, which is in reasonable agreement with the experimental value that was found for the same D−B−A systems (0.093 Å^{-1}). The strong initial decrease of the charge transfer rate with distance can be explained by considering the site energies shown in Figure 4. For the shortest bridge consisting of a single fluorene unit, the barrier height is relatively small (approximately 0.83 eV) due to the strong electrostatic interaction between negative and positive charges.

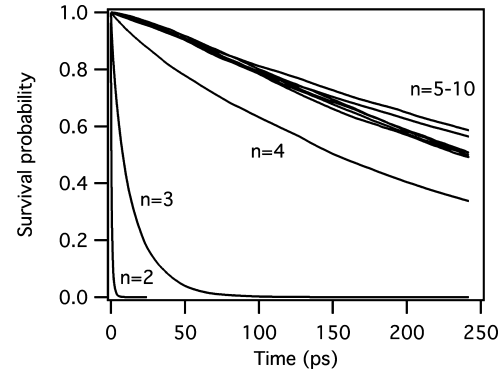

Figure 7. Survival probability as a function of time for D−B−A systems containing phenylene bridges of different lengths.

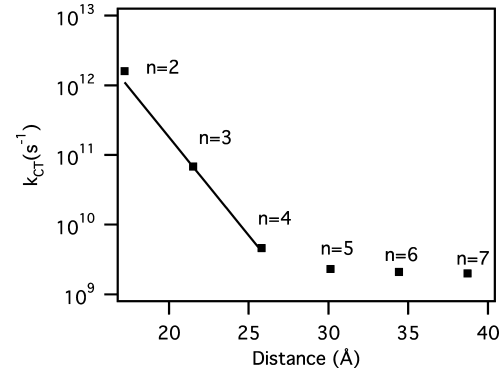

Figure 8. Charge transfer rate coefficient k_{CT} plotted against the distance between centers of donor and acceptor units in D−B−A systems with phenylene bridges. The solid line is an exponential fit to points with $n = 2-4$.

For the longer bridges, the barrier height gradually increases, leading to lower charge transfer rates. Note, however, that the effective barrier height changes less for longer bridges. As a result, the distance dependence of the charge transfer rate coefficient flattens off.

III.5. Dynamics of Charge Transfer: Phenyl Bridge. When the bridge consists of phenyl units, similar effects are observed as for the fluorene bridges above. In this case simulations were carried out with a rotational diffusion time of 10 ps (the rotation time of benzene in solution). The survival probability for the phenyl-based D−B−A systems is plotted as a function of time for bridges consisting of 1−10 phenyl units in Figure 7. The length of the longest bridge is similar to that of the longest fluorene based D−B−A system. Up to a length of four phenyl units the rate of charge transfer rapidly decreases but after that, up to 10 units, the rates are more or less constant. This is even more evident from Figure 8 where the rate is plotted against the distance between the donor and the acceptor. For the short bridges a strong exponential decrease with chain length is observed, as indicated by the fit in Figure 8. The value for β derived from this fit is 0.65 Å^{-1}, which is larger than the experimental value of 0.46 Å^{-1} for these systems.[34] After the fourth phenyl is added in the bridge, the rate of charge transfer does not decrease anymore with increasing bridge length and remains almost constant in qualitative agreement with the experimental data.[34] Unfortunately, there are no additional experimental data for longer D−B−A systems, but similar changes in the distance dependence of k_{CT} have been observed for other systems, for instance, for DNA-based systems.[42]

III.6. Charge Distribution on the D−B−A System during Charge Transfer. To gain insight into the mechanism of charge transfer, we have evaluated the charge density on the D−B−A

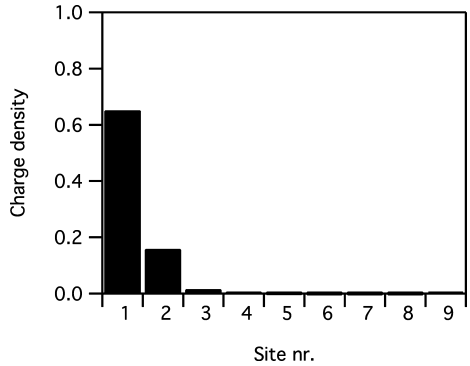

Figure 9. Charge distribution for a D−B−A system with a bridge consisting of 7 phenyl units.

system during charge transfer. In Figure 9 the total charge density on each of the bridge sites is shown for a D−B−A system in which the bridge consists of seven phenyl units. The charge density is highest on the hole donor (PDI, unit 1). This is not surprising since this unit has the lowest site energy. The density on the first bridge site is also considerable. On this site the positive charge is relatively close to the PDI^- and the electrostatic interaction is still quite strong here, resulting in the lower site energy (see Figure 4). For other bridge units, the site energy turns out to be considerably higher. This leads to a much lower average charge density on these sites during charge transfer. On the hole acceptor the charge decays irreversibly, as discussed above, and hence the charge density is negligible here. From the computational data on charge densities and on the distance dependence of charge transfer shown in Figures 6 and 8 we conclude that the electrostatic interaction between the hole on the bridge and the negative charge on the hole donor plays a significant role in the strong distance dependence of k_{CT} for short bridges. This dependence of the average bridge energy on the length of the bridge strengthens the distance dependence of the charge transfer coefficient that is already observed for rectangular bridges of increasing length. For these short bridges, holes can be transferred from D to A mainly via a single step tunneling mechanism, although some positive charge may build up on the bridge. For longer bridges, this tunneling process becomes so slow that it becomes dominated by a mechanism in which the bridge is populated. This population is always very small and the charge slowly leaks through the bridge toward the acceptor. Therefore, the latter mechanism is not a familiar hopping that suggests the charge localization on the bridge. Instead, sequential incoherent hopping is induced by dynamic fluctuations associated with torsion motion of bridge subunits. In separate calculations, in which the rotational diffusion is switched off and hence dynamic fluctuations are "frozen", the charge transfer rate was found to decrease strongly for the longer D−B−A systems also. This corresponds to previous results that we have obtained for charge transfer in donor−DNA−acceptor systems.[42] In this case the limiting rate of charge transfer is not determined by the mobility of charges along the bridge but by the rate of population of the bridge. This population rate is very small because of the large "injection barrier". If the limiting process would be the motion of the charge once it is on the bridge, the rate would be much faster. The mobility of charge along conjugated chains has been shown to be very high. For instance, a value of $\sim$60 $cm^2\ V^{-1}\ s^{-1}$ has been reported for polyfluorene.[44] This means that, once the charge is on the bridge, it migrates almost infinitely fast over the bridge (or back to the donor).

IV. Conclusions

We have theoretically studied the charge transfer in donor-bridge acceptor systems using a tight-binding model. In these calculations the effects of electrostatic interactions between the positive charge that is injected in the bridge and the negative charge that stays behind on the hole donor is accounted for. Moreover, we have explicitly included dynamic fluctuations by accounting for the rotational diffusion of the individual units. It is shown that the electrostatic interactions cause the strong distance dependence for short chains. For longer chains the charge transfer rate becomes weakly dependent on the distance between the donor and acceptor. In this regime the rate of charge transfer is determined by rate at which the charge moves from the donor to the bridge. The charge does not become fully localized on the bridge, illustrating that the mechanism is not a familiar hopping of temporary localized charges. However, it has also been found that dynamic fluctuations play a large role. In the absence of such fluctuations, the charge transfer rate continues to decrease rapidly for longer bridges.

References and Notes

(1) Kilså, K.; Kajanus, J.; Macpherson, A. N.; Mårtensson, J.; Albinsson, B. *J. Am. Chem. Soc.* **2001**, *123*, 3069–3080.
(2) Balzani, V.; Credi, A; Venturi, M. *ChemPhysChem* **2003**, *3*, 49–59.
(3) Weiss, E. A.; Wasielewski, M. R.; Ratner, M. A. *Top. Curr. Chem.* **2005**, *257*, 103–133.
(4) de Silva, A. P.; Leydet, Y.; Lincheneau, C.; McCleneghan, N. D. *J. Phys.: Condens. Matter* **2006**, *18*, S1847–S1872.
(5) Pischel, U. *Angew. Chem., Int. Ed.* **2007**, *46*, 4026–4040.
(6) Durrant, J. R.; Haque, S. A.; Palomares, E. *Coord. Chem. Rev.* **2004**, *248*, 1247–1257.
(7) Durrant, J. R.; Haque, S. A.; Palomares, E. *Chem. Commun.* **2006**, 3279–3289.
(8) Hagfeldt, A.; Boschloo, G.; Lindström, H.; Figgemeister, E.; Holmberg, A.; Aranyos, V.; Magnusson, E.; Malmqvist, L. *Coord. Chem. Rev.* **2004**, *248*, 1501–1509.
(9) Hagfeldt, A.; Grätzel, M. *Chem. Rev.* **1995**, *95*, 49–68.
(10) Hagfeldt, A.; Grätzel, M. *Acc. Chem. Res.* **2000**, *33*, 269–277.
(11) Hasselman, G. M.; Watson, D. F.; Stromberg, J. R.; Bocian, D. F.; Holten, D.; Lindsey, J. S.; Meyer, G. J. *J. Phys. Chem. B* **2006**, *110*, 25430–25440.
(12) Huber, M. *Eur. J. Org. Chem.* **2001**, *23*, 4379–4389.
(13) Lomoth, R.; Magnusson, A.; Sjödin, M.; Huang, P.; Styring, S.; Hammarström, L. *Photosynth. Res.* **2006**, *87*, 25–40.
(14) Noy, D.; Moser, C. C.; Dutton, P. L. *Biochim. Biophys. Acta Bioenerg.* **2006**, *1757*, 90–105.
(15) Song, H. E.; Kirmaier, C.; Schwartz, J. K.; Hindin, E.; Yu, L. H.; Bocian, D. F.; Lindsey, J. S.; Holten, D. *J. Phys. Chem. B* **2006**, *110*, 19121–19130.
(16) Song, H. E.; Kirmaier, C.; Schwartz, J. K.; Hindin, E.; Yu, L. H.; Bocian, D. F.; Lindsey, J. S.; Holten, D. *J. Phys. Chem. B* **2006**, *110*, 19131–19139.
(17) Wasielewski, M. R. *J. Org. Chem.* **2006**, *71*, 5051–5066.
(18) Miller, J. R.; Calcaterra, L. T.; Closs, G. L. *J. Am. Chem. Soc.* **1984**, *106*, 3047–3049.
(19) Jordan, K. D.; Paddon-Row, M. N. *Chem. Rev.* **1992**, *92*, 395–410.
(20) Wasielewski, M. R. *Chem. Rev.* **1992**, *92*, 435–461.
(21) Pullen, S. H.; Edington, M. D.; Studer-Martinez, S. L.; Simon, J. D. *J. Phys. Chem. A* **1999**, *103*, 2740–2743.
(22) Warman, J. M.; De Haas, M. P.; Verhoeven, J. W.; Paddon-Row, M. N. *Adv. Chem. Phys.* **1999**, *106*, 571–601.
(23) Wegewijs, B.; Verhoeven, J. W. *Adv. Chem. Phys.* **1999**, *106*, 221–264.
(24) Sikes, H. D.; Smalley, J. F.; Dudek, S. P.; Cook, A. R.; Newton, M. D.; Chidsey, C. E. D.; Feldberg, S. W. *Science* **2001**, *291*, 1519–1523.
(25) Walters, K. A.; Kim, Y.-J.; Hupp, J. T. *J. Electroanal. Chem.* **2003**, *554−555*, 449–458.
(26) Hviid, L.; Verhoeven, J. W.; Brouwer, A. M.; Paddon-Row, M. N.; Yang, J. X. *Photochem. Photobiol. Sci.* **2004**, *3*, 246–251.
(27) Weiss, E. A.; Ahrens, M. J.; Sinks, L. E.; Ratner, M. A.; Wasielewski, M. A. *J. Am. Chem. Soc.* **2004**, *126*, 9510–9511.
(28) Berlin, Y. A.; Grozema, F. C.; Siebbeles, L. D. A.; Ratner, M. A. *J. Phys. Chem. C* **2008**, *112*, 10988–11000.

(29) For review see: (a) Schatz, G. C.; Ratner, M. A. *Quantum Mechanics in Chemistry*; Prentice Hall: Englewood Cliffs, NJ, 1993. (b) Barbara, P. F.; Meyer, T. J.; Ratner, M. A. *J. Phys. Chem.* **1996**, *100*, 13148–13168. (c) Ratner, M. A.; Jortner, J. *Molecular Electronics*; Blackwell: Oxford, U.K., 1997. (d) Bixon, M.; Jortner, J. *Adv. Chem. Phys.* **1999**, *106*, 35–202. (e) Kuznetsov, A. M.; Ulstrup, J. *Electron Transfer in Chemistry and Biology*; Wiley: Chichester, U.K., 1999. (f) Balzani, V., Piotrowiak, P., Rodgers, M. A. J.; Mattay, Z., Astruc, D., Gray, H. B., Winkler, J., Fukuzumi, S., Mallouk, T. E., Haas, Y., de Silva, A. P., Gould, I., Eds. *Electron Transfer in Chemistry*; Wiley-VCH Verlag GmbH: Weinheim, 2001; Vols. *1*−*5*. (g) Adams, D. M.; Brus, L.; Chidsey, C. E. D.; Creager, S.; Creutz, C.; Kagan, C. R.; Kamat, P. V.; Lieberman, M.; Lindsay, S.; Marcus, R. A.; Metzger, R. M.; Michel-Beyerle, M. E.; Miller, J. R.; Newton, M. D.; Rolison, D. R.; Sankey, O.; Schanze, K. S.; Yardley, J.; Zhu, X. *J. Phys. Chem. B* **2003**, *107*, 6668–6697. (h) Berlin, Y. A.; Kurnikov, I. V.; Beratan, D.; Ratner, M. A.; Burin, A. L. *Top. Curr. Chem.* **2004**, *237*, 1–36.

(30) Kittel, C. *Introduction to Solid State Physics*, 7th ed.; John Wiley: New York, 1996.

(31) Gutman, F.; Lyons, L. E. *Organic Semiconductors*; John Wiley: New York, 1966.

(32) Segal, D.; Nitzan, A.; Davis, W. B.; Wasielewski, M. R.; Ratner, M. A. *J. Phys. Chem. B* **2000**, *104*, 3817–3829. Berlin, Y. A.; Burin, A. L.; Ratner, M. A. *J. Phys. Chem. A* **2000**, *104*, 443–445. Berlin, Y. A.; Burin, A. L.; Ratner, M. A. *J. Am. Chem. Soc.* **2001**, *123*, 260–268. Wang, X.; Nau, W. M. *ChemPhysChem.* **2001**, *2*, 761–766. Nitzan, A. *Annu. Rev. Phys. Chem.* **2001**, *52*, 681–750. Bicout, D. J.; Kats, E. *Phys. Lett. A* **2002**, *300*, 479–484. Nitzan, A. *Isr. J. Chem.* **2002**, *42*, 163–166. Petrov, E. G.; Shevchenko, Ye. V.; May, V. *Chem. Phys.* **2003**, *288*, 269–279.

(33) Berlin, Y. A.; Burin, A. L.; Ratner, M. A. *Chem. Phys.* **2002**, *275*, 61–74.

(34) Weiss, E. A.; Ahrens, M. J.; Sinks, L. E.; Gusev, A. V.; Ratner, M. A.; Wasielewski, M. R. *J. Am. Chem. Soc.* **2004**, *126*, 5577–5584.

(35) Goldsmith, R. H.; Sinks, L. E.; Kelley, R. F.; Betzen, L. J.; Liu, W.; Weiss, E. A.; Ratner, M. A.; Wasielewski, M. R. *Proc. Natl. Acad. Sci. U.S.A.* **2005**, *102*, 3540–3545.

(36) Lewis, F. D.; Zhu, H.; Daublain, P.; Cohen, B.; Wasielewski, M. R. *Angew. Chem., Int. Ed.* **2006**, *45*, 7982–7985.

(37) Lewis, F. D.; Zhu, H.; Daublain, P.; Fiebig, T.; Raytchev, M.; Wang, Q.; Shafirovich, V. *J. Am. Chem. Soc.* **2006**, *128*, 791–800.

(38) Grozema, F. C.; Berlin, Y. A.; Siebbeles, L. D. A. *J. Am. Chem. Soc.* **2000**, *122*, 10903–10909.

(39) Grozema, F. C.; van Duijnen, P. T.; Berlin, Y. A.; Ratner, M. A.; Siebbeles, L. D. A. *J. Phys. Chem. B* **2002**, *106*, 7791–7795.

(40) Risken, H. *The Fokker-Planck Equation*; Springer-Verlag: Berlin, 1984.

(41) Weller, A. *Z. Phys. Chem. Neue Folge* **1982**, *133*, 93–98.

(42) Grozema, F. C.; Tonzani, S.; Berlin, Y. A.; Schatz, G. C.; Siebbeles, L. D. A.; Ratner, M. A. *J. Am. Chem. Soc.* **2008**, *130*, 5157–5166.

(43) Breneman, C. M.; Wiberg, K. B. *J. Comput. Chem.* **1990**, *11*, 361–373.

(44) Prins, P.; Grozema, F. C.; Galbrecht, F.; Scherf, U.; Siebbeles, L. D. A. *J. Phys. Chem. C* **2007**, *111*, 11104–11112.

JP1023422